Title
Resistivity and Induced Polarization Survey at a Russian Nuclear Waste Site

Author
Frangos, W.

Publication Date
1996

LBL-38188
UC-603
Preprint

Lawrence Berkeley Laboratory
UNIVERSITY OF CALIFORNIA

EARTH SCIENCES DIVISION

Submitted to Geophysics

Resistivity and Induced Polarization Survey at a Russian Nuclear Waste Site

W. Frangos and S. Ter-Saakian

January 1996

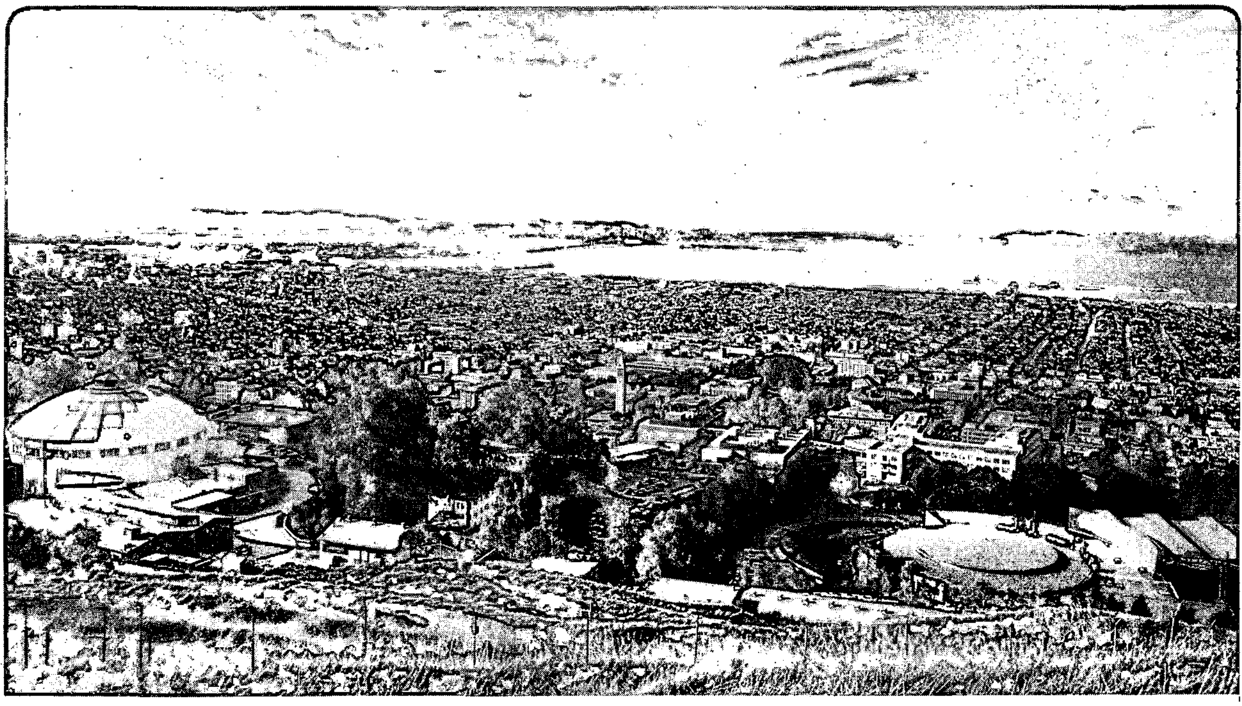

Prepared for the U.S. Department of Energy under Contract Number DE-AC03-76SF00098

DISCLAIMER

LBL-38188
UC-603

Resistivity and Induced Polarization Survey at a Russian Nuclear Waste Site

William Frangos* and Sergei Ter-Saakian**

*Earth Sciences Division
Ernest Orlando Lawrence Berkeley National Laboratory
University of California
Berkeley, California 94720

**Hydrospetzgeologia, Moscow, Russia

January 1996

This work was supported in part by the Russian Ministry of Atomic Energy through P.A. Mayak, and jointly by the Office of Environmental Management, Office of Technology Development (EM-OTD), and the Office of Energy Research, Office of Basic Energy Sciences (ER-BES), of the U.S. Department of Energy under Contract No. DE-AC03-76SF00098.

ABSTRACT

Electrical resistivity and induced polarization (IP) data from the area of a radioactive and nitrate-rich groundwater plume were gathered by a joint Russian-American team. The results show the contaminated area both to be conductive and to have an anomalously low IP response. The low IP response may be due to a radiolytic reaction with the dissolved nitrate, yielding oxygen which, in turn, reacts to remove accessory pyrite from the host rocks.

INTRODUCTION

The P.A. Mayak plant near Chelyabinsk, Russia (Figure 1) has produced weapons grade fissionable materials since the 1940s. An unfortunate series of mishaps has resulted in a variety of environmental problems, including the loss of acidic, radioactive waste products into the groundwater in a remote area between Lake Karachai and the River Mishelyak.

An electrical resistivity and induced polarization survey was undertaken as part of a joint Russian-American effort to study the problem. The work described here was conducted between 10 and 18 September 1994. Purposes of the work were 1) to characterize the subsurface groundwater flow regime, and 2) to determine whether the Mayak contaminant plume may be mapped by surface electrical geophysical methods. The first purpose is important as a means of predicting the migration of contaminants from Lake Karachai toward the Mishelyak River. The second is thought plausible in that the contaminated groundwater has been reported to have a nitrate concentration so high as to yield a resistivity of about 0.1 Ω-m, as contrasted with more usual groundwater resistivities in the area of 10 to 100 Ω-m.

Successful results have been obtained tracing contaminant plumes as conductive features using various surface electrical and electromagnetic methods (e.g., Ross, et al., 1990; Buselli, et al., 1990; Goldstein, et al., 1990). Induced polarization (IP) represents an additional parameter which may be employed to characterize subsurface electrical properties (e.g., Sandberg, 1991; Seara and Granda, 1987; Soinenen and Vanhala, 1992). Accordingly, we decided to gather IP data at the Mayak site to evaluate its usefulness in tracing the nitrate plume.

GEOLOGICAL SETTING

Geological information is based upon reports by Russian workers in the area, (Drozhko, et al., 1993; Solodov, et al., 1994) and on observations by other members of the field party (Drozhko, et al., 1996). In general, the water in DH 176 is strongly contaminated, while that in DH 173 is clean.

Bedrock throughout the region is described as a "porphyrite", a low-grade metamorphosed porphyritic andesitic to basaltic assemblage of flows, volcaniclastics, and shallow intrusives. As observed in both the drillholes and in a nearby quarry, the porphyrite is irregularly silicified, epidotized, and calcified. These styles of alteration tend to make a rock more resistive by decreasing porosity and the interconnectivity of pore spaces. Exposures in the quarry show that weathering depths are highly variable, ranging between nil and 10 or so meters. A near-vertical set of fractures and a nearly horizontal one are reported from outcrop exposures.

The overburden in the area generally consists of a loamy, clayey soil which was generally moist at the time of this work. Depth of bedrock below surface is noted to be 3.4 meters in drillhole 176 and nil to 1.3 meters in drillhole 173, as indicated in the cross-section, Figure 2. Such thin layers (compared to the dipole length) of overburden have a nearly negligible effect on apparent resistivity.

SURVEY PROCEDURES

Figure 3 shows the locations of the lines surveyed with respect to the topography and selected drillholes in the area. Components of the survey were positioned to take advantage of drillhole control, while avoiding interference from cultural features such as pipelines and drill casings. Profile A runs along the longer geologic cross section of Figure 2, between drillholes 43/78 and 173, through drillhole 176, site of extensive logging and packer tests (Drozhko, et al., 1996). Profile B is situated south of the Mishelyak River, in an area thought to lie beyond the present extent of the contaminant plume. Profile C runs along the trend of the contaminant plume, traversing the other two profiles, with a large gap due to inaccessible marshes along the river. Much of the region south of the Mishelyak River is covered with fly ash from a nearby coal-fired power plant.

A 20-m conventional dipole-dipole array was employed throughout the survey, in order to gather both sounding and profiling information simultaneously. Results are plotted in pseudosection format, with apparent resistivity presented in ohm-meters (Ω-m) and apparent IP effect shown as phase lag in milliradians (mR). Locations were determined with reference to known drillholes and, occasionally, by Brunton compass sightings to recognized features. A few GPS readings served as checks on overall location. Electrode intervals were measured with a standard field wire, measured with a tape and cut to length at the beginning of the work. Directions along lines were determined Brunton and by backsighting.

Equipment used consisted of a phase-measuring IP and resistivity receiver and a portable, battery-powered transmitter. The instrumentation is based on a stable oscillator clock which provides a phase reference system (Frangos, 1990). The entire survey was conducted at a frequency of 1 Hz. Porous pot receiver electrodes were employed throughout, while transmitter electrodes were single metal stakes. Overall precision of apparent resistivity measurements depends upon relative accuracy of electrode locations and the determination of current and voltage; the precision is estimated to be ±4% or better. Phase measurements are generally accurate to ±1 mR.

Results

Profile A, with its west end, station 17W, about 2 meters east of DH 43/78, runs past DH 176 at the midpoint of dipole 1-2W, to within about 5 m of a slurry pipeline, about 20 m northwest of DH 173. The data are presented as the pseudosection of Figure 4. Slight mismatches between data from overlapping segments of the line are not unexpected since the stations do not coincide exactly.

Higher apparent resistivities occur on the east and west ends of the line, with relatively low apparent resistivities in the middle portion. The high apparent resistivities are associated with outcrops of porphyrite between stations 12E and 14E and in the small hill near dipole 13-14W (not shown on the geologic cross section). Apparent IP responses vary similarly as the apparent resistivity, with two exceptions: at the extreme east end of the profile where a number of negative apparent IP effects are noted, and in the region between stations -3 and -10 where relatively high IP values are associated with low apparent resistivities. The slightly negative apparent IP effects on the east are interpreted as a normal geometric effect associated with the sharp resistivity contrast.

Profile B

Surveyed in two sections, Profile B serves to define background responses of the soil and bedrock in an area presumably well away from the contaminant plume. The eastern portion of Profile B is situated on a berm between the fly ash-covered region and the swamps south of the Mishelyak; the log of drillhole DH 3,77 reports about 4 meters of fly ash and 11 meters of soil and sediment overlying porphyrite bedrock at a depth of 15 meters. The eastern portion traverses an area of normal soil cover.

The results, Figure 5, show a nearly classic layered earth resistivity and IP pattern to the east. Care was taken to avoid data contamination from the drill casing of DH 3,77; we were at least partially successful in this effort. Note that the porphyrite underlying the fly ash and sediments is both resistive and IP responsive at this location. Apparent resistivities on the western portion of the profile suggest conductive soils at the extremes of the segment and a buried ridge of resistive bedrock at depth near the center. Apparent IP effects are moderate throughout, increasing slightly to the southeast.

Profile C

The southern segment of Profile C is placed along a track through the marshy fly-ash, while the northern portion extends away from DH 176. The intervening area is only accessible when the river and marsh are frozen. A pair of drillholes are situated at station -29.

On the south end, the data (Figure 6) reveal a pattern similar to that seen on the east end of Profile B: low apparent resistivities and IP effects at shallow separations overlying higher resistivities and IP effects. The drillstems appear to have disrupted the data, yielding a less ideal layered-earth pattern in the results. To the north, apparent resistivity is generally high, and IP effects are quite low.

DISCUSSION

General Characteristics

The survey results indicate that fresh bedrock at the P.A. Mayak site is highly resistive, 500 to over 1,000 Ω-m. The overburden, on the other hand, is more conductive; 50 Ω-m appears to be representative. The fly ash, a special case, is highly conductive at less than 10 Ω-m. The intrinsic IP effects of the soil and fly ash typically exhibit a background response of 8 to 10 mR, owing to the minor clay content, while the IP response of the bedrock appears variable.

Measurements of water resistivity in drillhole 176 show "specific resistance" in the range 8 to 15 Ω-m. Lower resistivities correspond to higher ion content. Samples of ground water have shown resistivities as low as 0.1 Ω-m due to nitrate contamination.

The resistivity of saturated rock, to a first order approximation or better, is a linear function of pore-water resistivity, as expressed in Archie's Law, (Archie, 1942)

$$\rho_{rock} = \rho_{water}\phi^{-m}$$

in which ϕ is the porosity of the rock,

and m is the "cementation factor," an empirical constant generally about 2

Water resistivity, at near-surface temperatures and pressures, is primarily a function of salinity or ion content. Porosity of igneous and metamorphic rocks such as the porphyrite may be taken to lie in the range of 1 to 10% in the absence of fractures, and higher in fracture zones. The relative influences of water resistivity and rock porosity on total rock resistivity are seen to be similar, since water resistivity may vary through several orders of magnitude, while porosity acts as the second power.

In light of the above considerations, there are three main possible causes of low apparent resistivities in the survey data:

1) decreased bedrock resistivity due to high fracture density, the fractures being filled with contaminated, relatively conductive ground water,
2) decreased resistivity of low- to moderate fracture density bedrock due to invasion by extremely conductive contaminated ground water, and,
3) thickening of the conductive overburden layer.

Thus areas of low resistivity bedrock are significant either as potential conduits for contaminant flow or regions into which contaminated ground water has already moved.

Numerical Models of the Results

A series of two-dimensional numerical models was calculated which aid interpretation of the survey results. Figure 7 shows four models in section view: the first represents a 10-m layer of conductive overburden lapping onto resistive bedrock, the second is the same with the addition of a 5-m depression on the bedrock surface, while the third adds a 20-m wide conductive fracture zone in the bedrock. Figures 8, 9, 10, and 11 present the apparent resistivity and IP effects which would be observed over these structures. Figure 8 shows an apparent resistivity pattern similar to those obtained on the east end of Profile A. Note the decreased IP response at the extreme end of the model, correlating with the region of negative apparent IP effect at the east end of the profile. Variable bedrock topography or depth of weathering, as modeled in Figure 9, can account for some of the variations. Note the similarity between Figure 10 and the observed resistivity data of the east end of Profile A (Figure 4). The model indicates that bedrock itself at DH 176 is highly conductive, since the drillhole encountered porphyrite at a depth of only 3.4 m. The high number of fractures noted in the drillhole is consistent with this finding.

The fly ash cover encountered on Profiles B and C poses a special problem, in that it acts as a conductive cover, shielding the underlying material from investigation. The fourth numerical model (Figure 7) is relevant to the eastern segment of Profile B; a conductive layer overlies a resistive and IP responsive basement which may or may not contain a conductive, non-IP-responsive, vertical-standing fracture zone. In the absence of the fracture zone the results are perfectly layered; Figure 11 shows those in its presence. The numerical model is in good agreement with the observed results, suggesting that a fracture zone may be present at or just east of drillhole 3,77.

Implications of the IP Results

The relationship between IP response and the zone of known contamination is striking. Low apparent IP effects correlate with the regions of greater groundwater contamination, while the porphyrite bedrock in general appears to have an IP response of 5 to 12 mR. Such background response is not uncommon for metamorphosed volcanic rocks, which often contain significant accessory pyrite, magnetite, and cation-exchanging clays. The question at hand is why the IP response is decreased in the contaminated porphyrite. We speculate as follows.

Water samples from DH 176 showed relatively high oxygen concentrations (Solodov, et al., 1994). Pyrite is stable in acidic environments, but unstable in oxidizing environments, reverting to hydrous iron oxides and sulfuric acid. It has been suggested (John Apps, personal communication) that the excess oxygen may be generated by interaction between the radioactive contaminants and the nitric acid. This radiolytic reaction, along the lines of

$$2\ H_2NO_3 + (\text{gamma, alpha}) = N_2 + 2\ H_2O + 2\ O_2$$

could readily explain the observed strong correlation between low IP responses and the radioactive, nitrate-rich groundwater.

CONCLUSIONS AND RECOMMENDATION

Surface electrical resistivity measurements provide useful results in both characterizing the groundwater transport regime and tracing the flow of the contaminant plume. Induced polarization data at Mayak correlate well with the known extent of the plume in the sense of decreased IP response from the contaminated area. It appears that the radioactive, nitrate-rich groundwater removes accessory pyrite from the porphyrite host rocks, lowering the IP response. A further laboratory investigation of the hypothesized radiolytic decrease of IP response may be warranted.

ACKNOWLEDGEMENTS

This work was funded, on the Russian side, by the Russian Ministry of Atomic Energy through P.A. Mayak and, on the United States side, jointly by the Office of Environmental Management, Office of Technology Development (EM-OTD) and the Office of Energy Research, Office of Basic Energy Sciences (ER-BES) of the U.S. Department of Energy through the E.O.

Lawrence Berkeley National Laboratory under Contract Number DC-AC03-76SF00098. Dr. Chin-Fu Tsang made the arrangements which allowed this investigation to occur. The administration and staff of P.A. Mayak were of great assistance, providing, in addition to the basic access, numerous support services during the conduct of the field work. In particular, we express thanks for the efforts of E.Z. Drozhko and G. Romanov. The American team was ably headed up by Harold "Skip" Wollenberg. Discussions with John Apps of LBNL were very helpful. Katya Tashkova provided translation services, no mean feat.

LIST OF FIGURES

Fig. 1: Area Location Map, P.A. Mayak site, Chelyabinsk, Russia
Fig. 2: Geologic cross-section, Drillhole 43/78 through DH 173 and Profile B of Figure 3. (schematic vertical scale)
Fig. 3: Line Location Map
Fig. 4: Resistivity and IP Profile A, a = 20 m
Fig. 5: Resistivity and IP Profile B, a = 20 m
Fig. 6: Resistivity and IP Profile C, a = 20 m
Fig. 7: Sketch of Numerical Model Cases
Fig. 8: Numerical results for overburden lapping onto resistive basement
Fig. 9: Numerical results for overburden lapping onto resistive basement with buried valley
Fig. 10: Numerical results for overburden lapping onto resistive basement with buried valley and shear zone in basement
Fig. 11: Numerical results for ash over bedrock with a fracture zone in the basement

REFERENCES

Archie, G.E., 1942, The electrical resistivity log as an aid in determining some reservoir characteristics: A.I.M.E., Trans., **146**, 54–61

Buselli, G., Barber, C., Davis, G.B., and Salama, R.B., 1990, Detection of groundwater contamination near waste disposal sites with transient electromagnetic and electric methods, *in* Stanley H. Ward, Ed., Geotechnical and Environmental Geophysics: Soc. Expl. Geophys., Invest. Geophys., **5**, 27–39

Drozhko, E.G., Mokrov, Yu.G., Glagolenko, Yu.V., and Samsonova, L.M., 1993, Determination of hydrodynamic parameters of a cleaved rock mass according to regime examination data in the Lake Karachai area: *in preparation,* Chelyabinsk, Russia

Drozhko, E.G., Glagolenko, Y.U., Mokrov, Y.G., Ivanov, I.A., Postovalova, G.A., Samsonova, L.M., Glagolev, A.V., Ter-Saakian S.A., Glinsky, M.A., Vasil'kova, N., Skokov, A.V., Wollenberg, H.A., Tsang, C.-F., Frangos, W., Solbau, R.D., Stevenson, K., Lowder, W.M., and Foley, M.G., 1996, Joint Russian-American hydrogeological-geochemical studies on the Karachai-Mishelyak system, South Urals, Russia: *submitted to* Journal of Environmental Geology and Water Science

Frangos, W., 1990, Stable-oscillator phase IP systems, *in* James B. Fink, et al., Eds., Induced Polarization: applications and case histories: Soc. Expl. Geophys., Invest. Geophys **4**, 79–90

Goldstein, N.E., Benson, S.M., Alumbaugh, D.L., 1990, Saline groundwater plume mapping with electromagnetics, *in* Stanley H. Ward, Ed., Geotechnical and Environmental Geophysics: Soc. Expl. Geophys., Invest. Geophys., **5**, 17–25

Ross, H.P., Mackelprang, C.E., and Wright, P.M., 1990, Dipole-dipole electrical resistivity surveys at waste disposal study sites, *in* Stanley H. Ward, Ed., Geotechnical and Environmental Geophysics: Soc. Expl. Geophys., Invest. Geophys., **5**, 145–152

Sandberg, S.K., 1993, Examples of resolution improvement in geoelectrical soundings applied to groundwater investigations: Geophys. Prosp., **41**, 207–228

Seara, J.L., and Granda, A., 1987, Interpretation of IP time domain / resistivity soundings for delineating sea-water intrusions in some coastal areas of the northeast of Spain: Geoexploration, **24**, 153–167

Soinenen, H.T., and Vanhala, H., 1992, Spectral induced polarization method in mapping soils polluted by organic chemicals: Presented at 54th Ann. Internat. Mtg., Eur. Assn. Expl. Geophys.

Solodov, I.N., Velichkin, V.I., Zotov, A.V., Kochkin, B.T., Drozhko, E.G., Glagolev, A.V., and Skokov, A.N., 1994, Distribution and geochemistry of contaminated subsurface waters in fissured volcanogenic bedrock of the Lake Karachai area, Chalyabinsk, Southern Urals: Lawrence Berkeley National Laboratory report LBL-36780

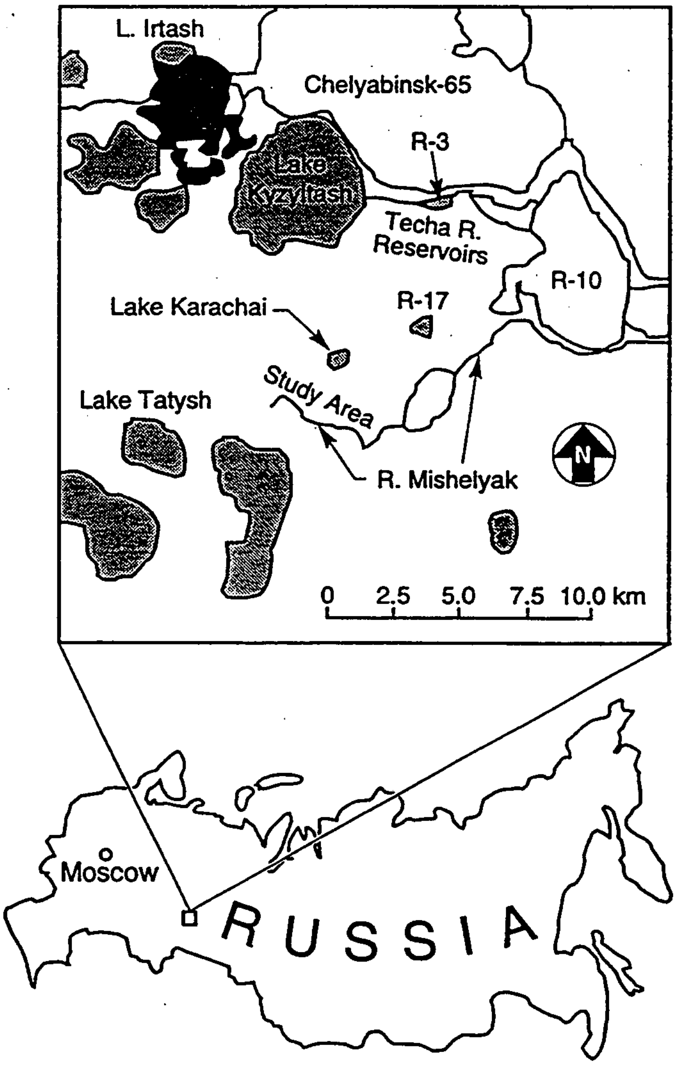

Chelyabinsk-65 Area

XBD 9510-05004.ILR

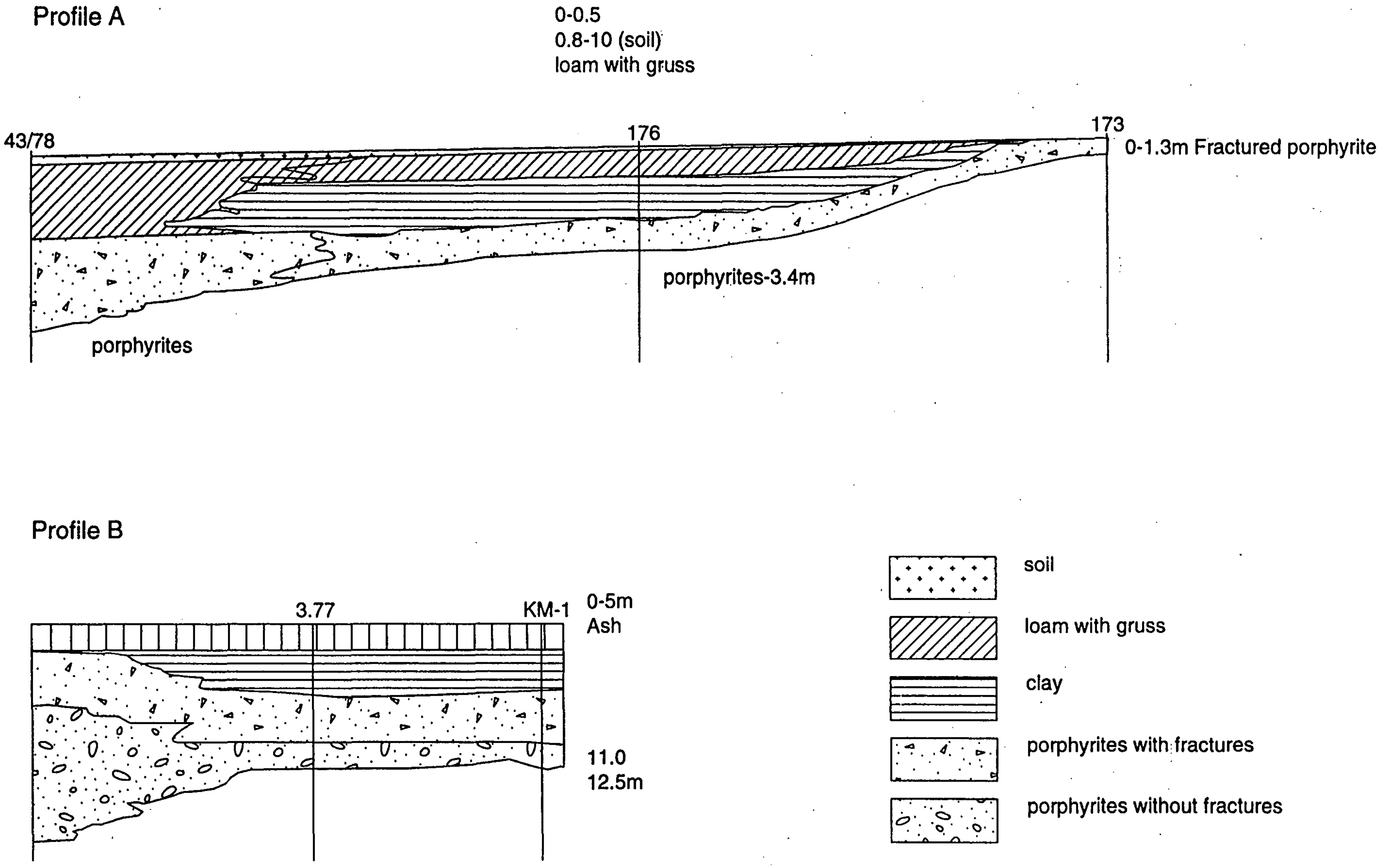

Fig 2 - Geologic cross sections

XBD 9511-05126.ILR

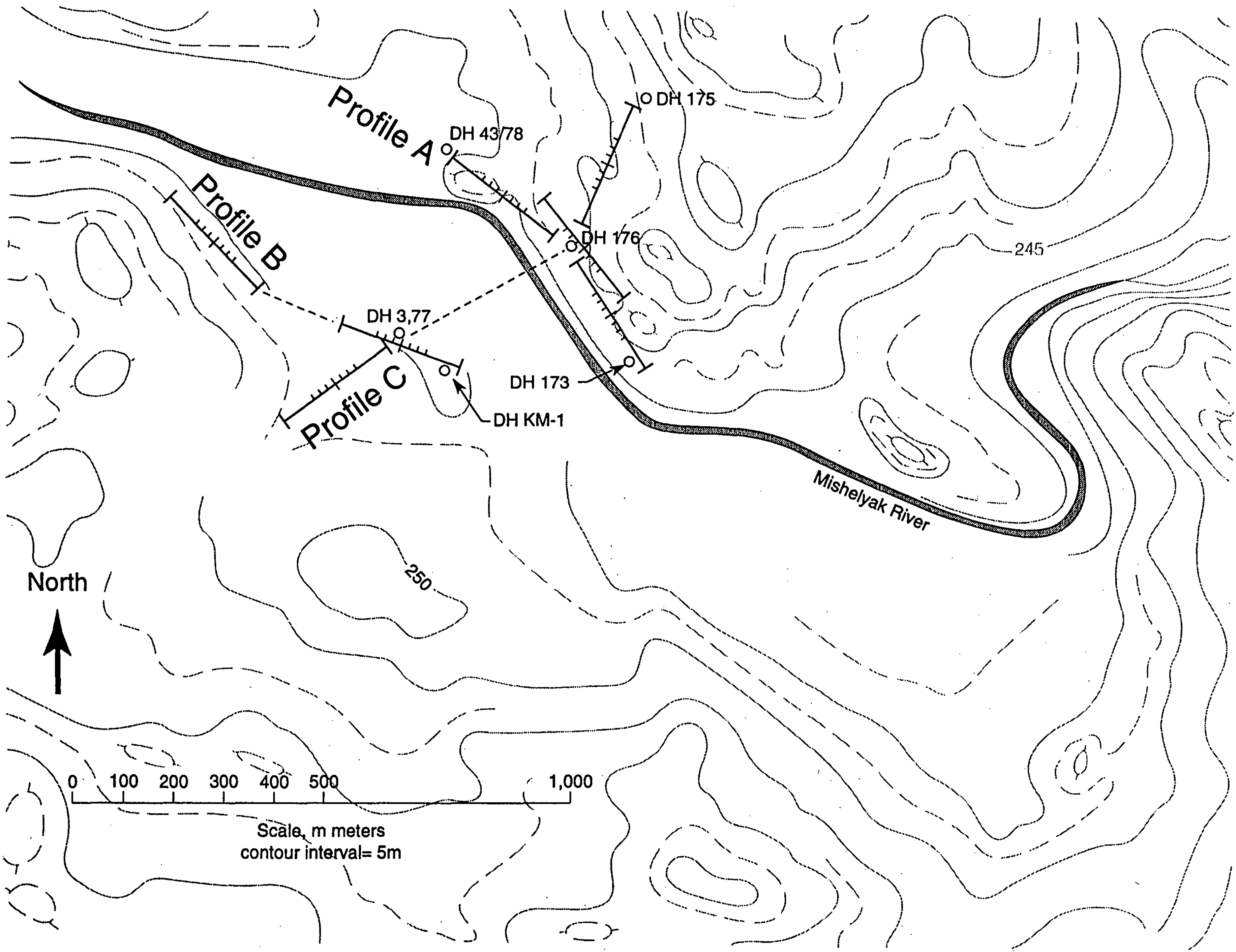

Figure 3: Line Location Map

XBD 9511-05127.ILR

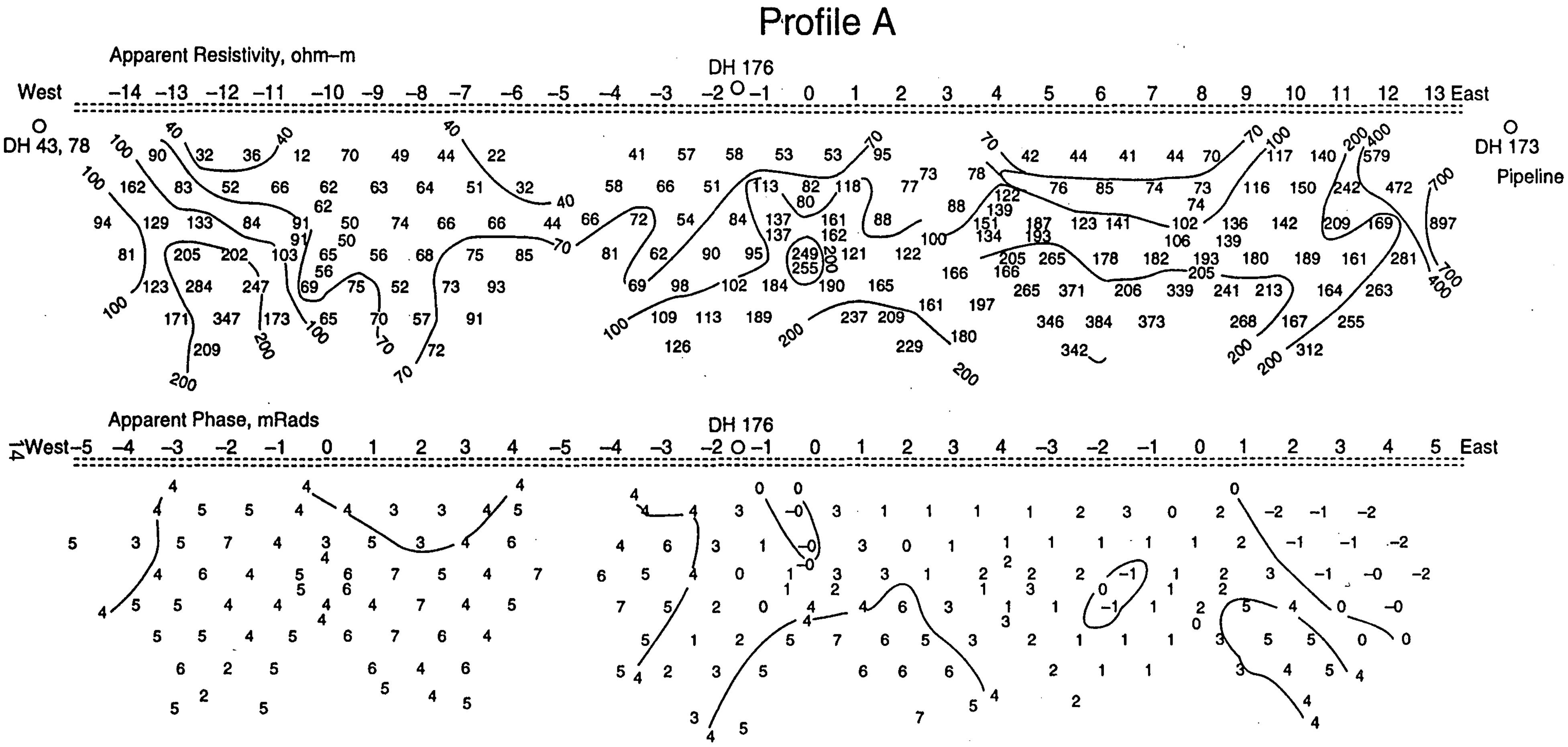

Fig. 4: Resistivity & IP data for Profile A.

DH 173XBD 9511-05128.ILR

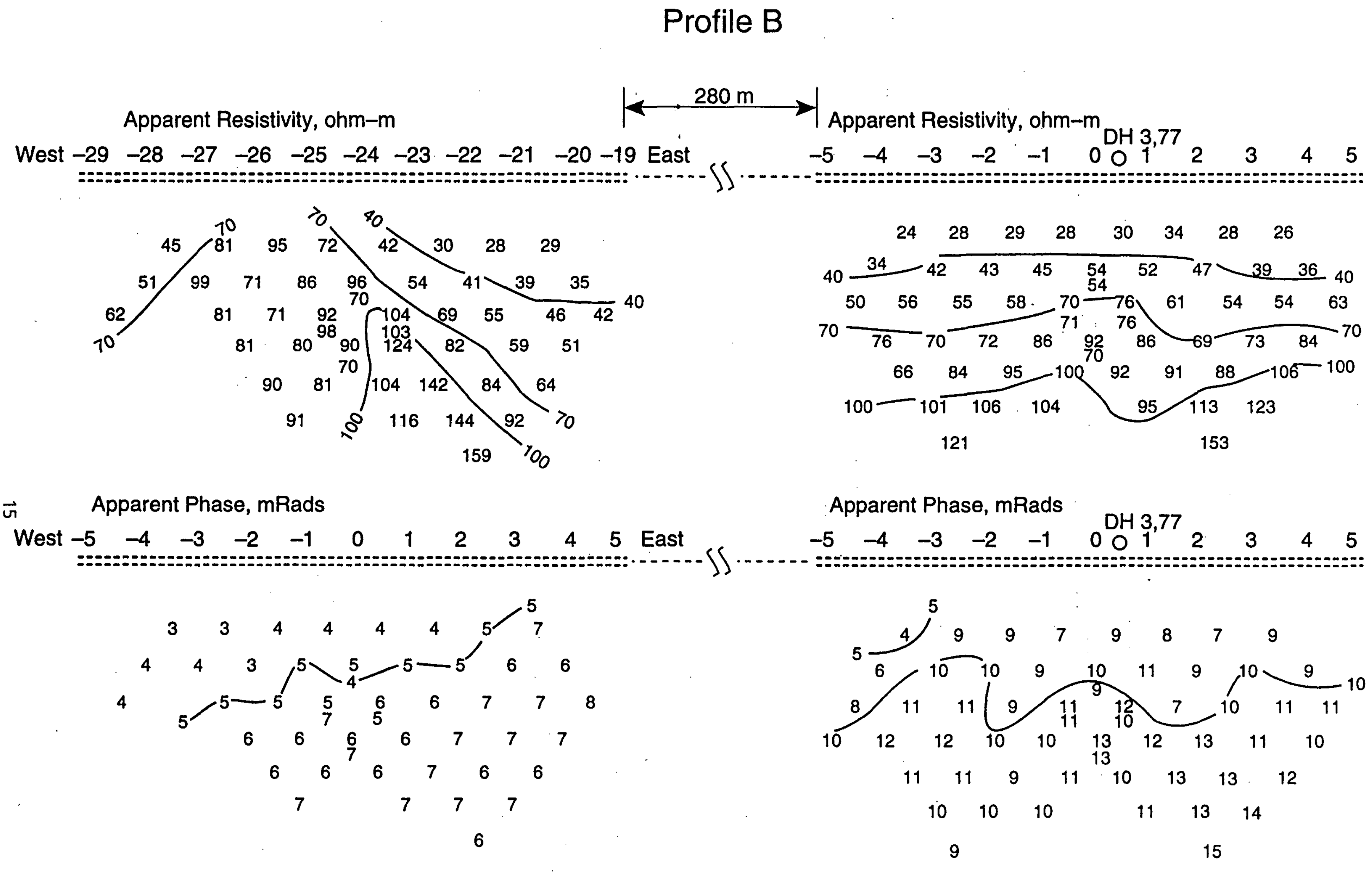

Fig. 5: Resistivity & IP data for Profile B.

XBD 9511-05129.ILR

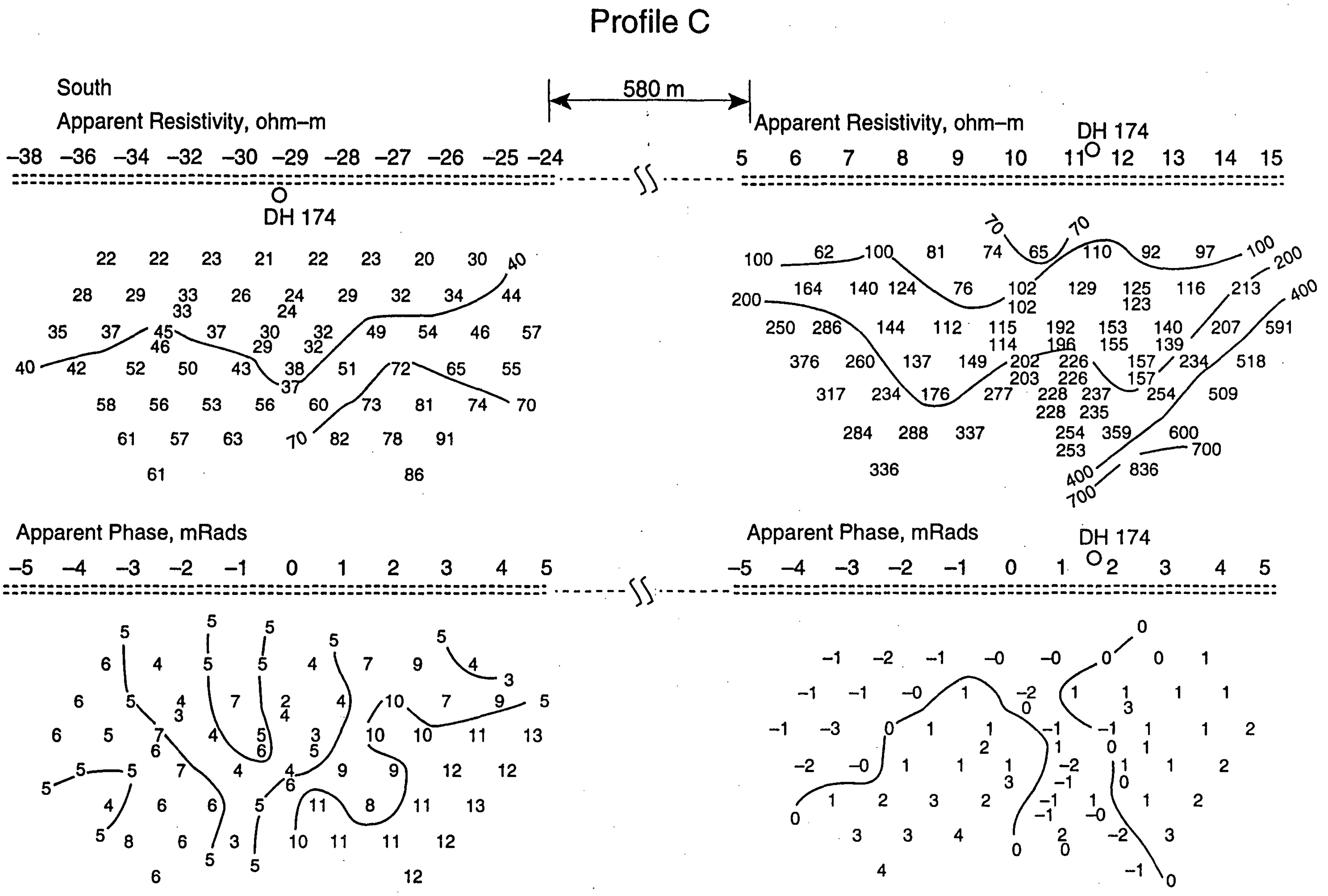

Fig. 6: Resistivity & IP data for Profile C.

XBD 9511-05130.ILR

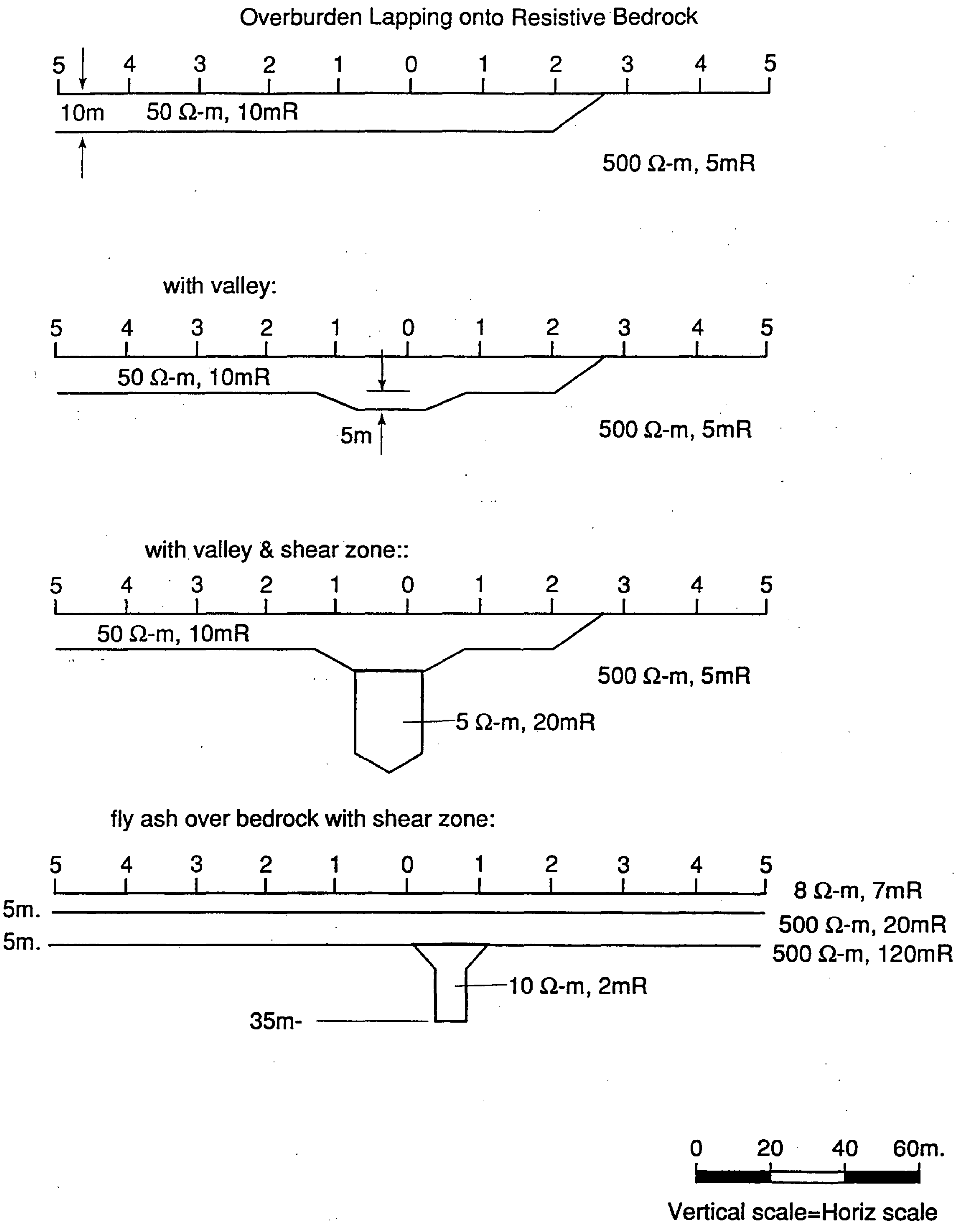

Fig. 7: Descriptions of numerical models

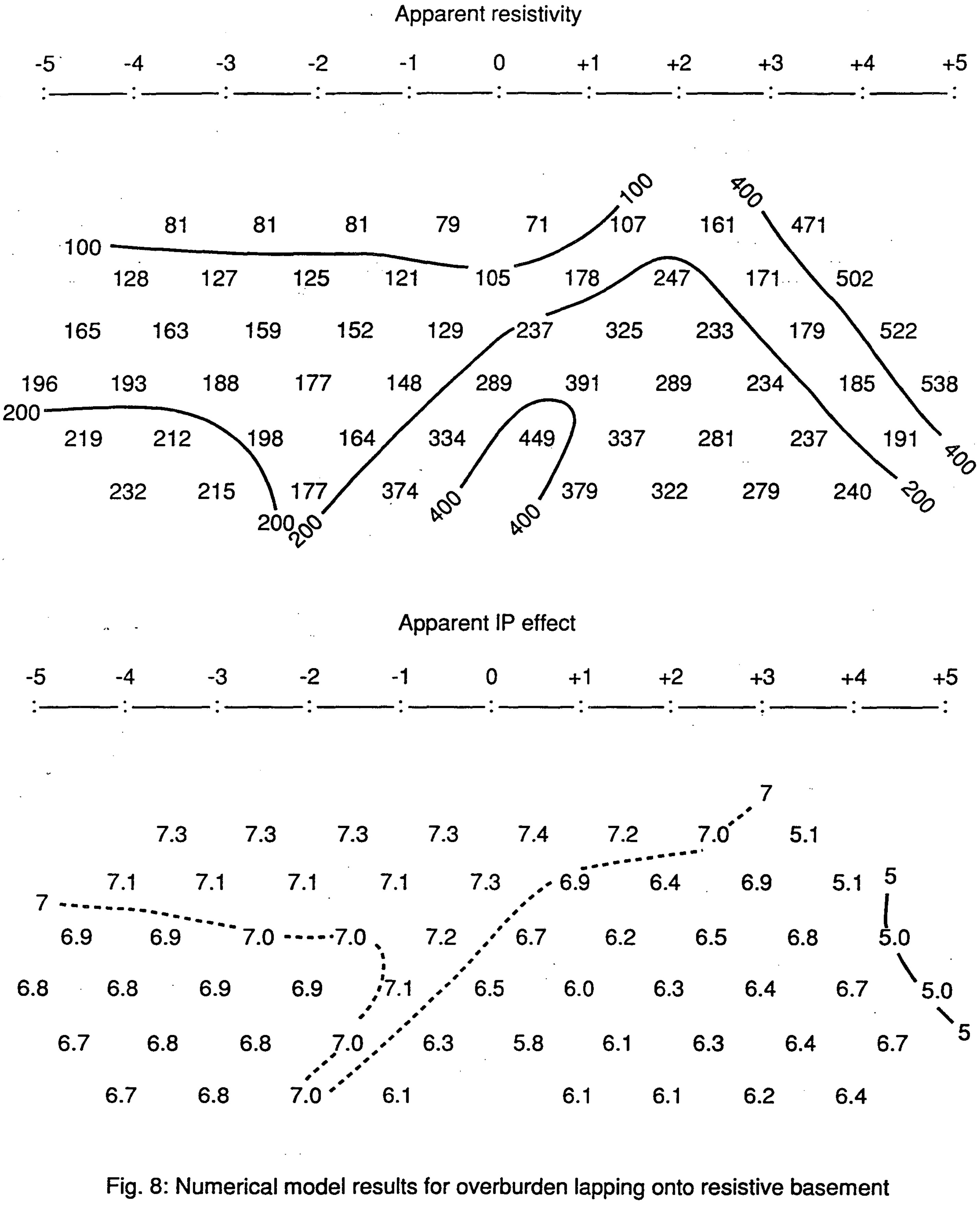

Fig. 8: Numerical model results for overburden lapping onto resistive basement

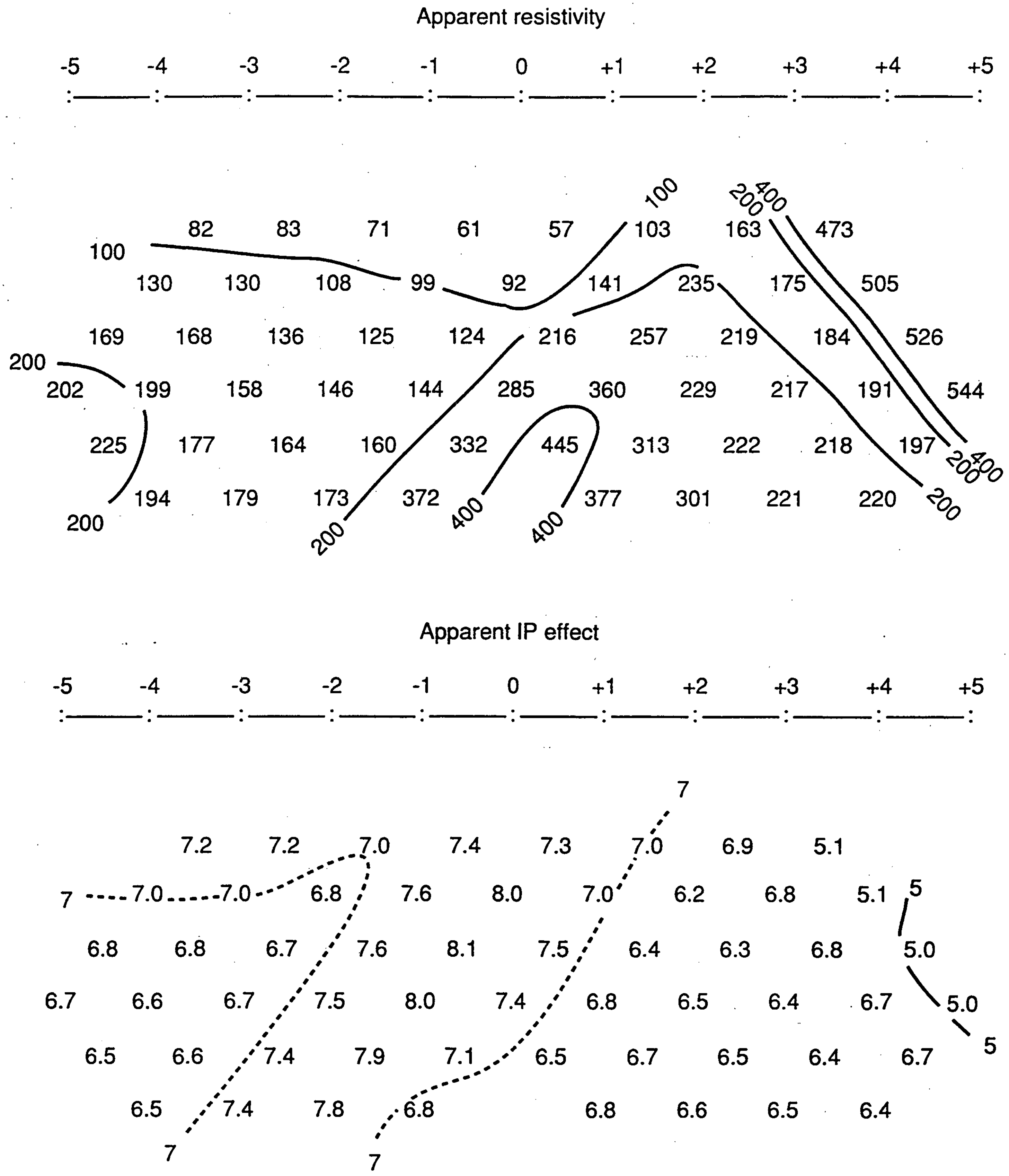

Fig. 9: Numerical model results for overburden lapping onto resistive basement, with buried valley

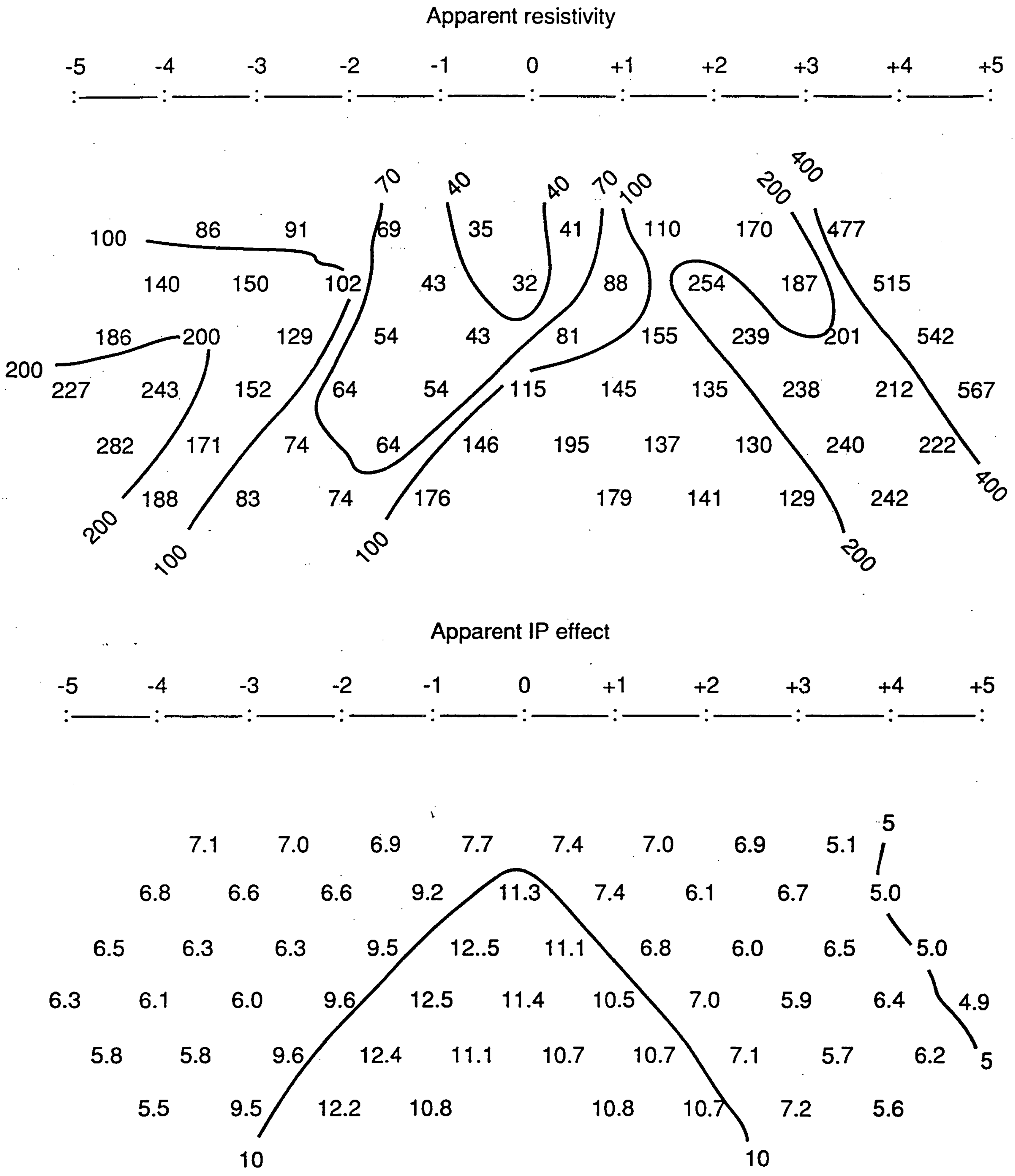

Fig. 10: Numerical model results for overburden lapping onto resistive basement, w/ valley & shearzone

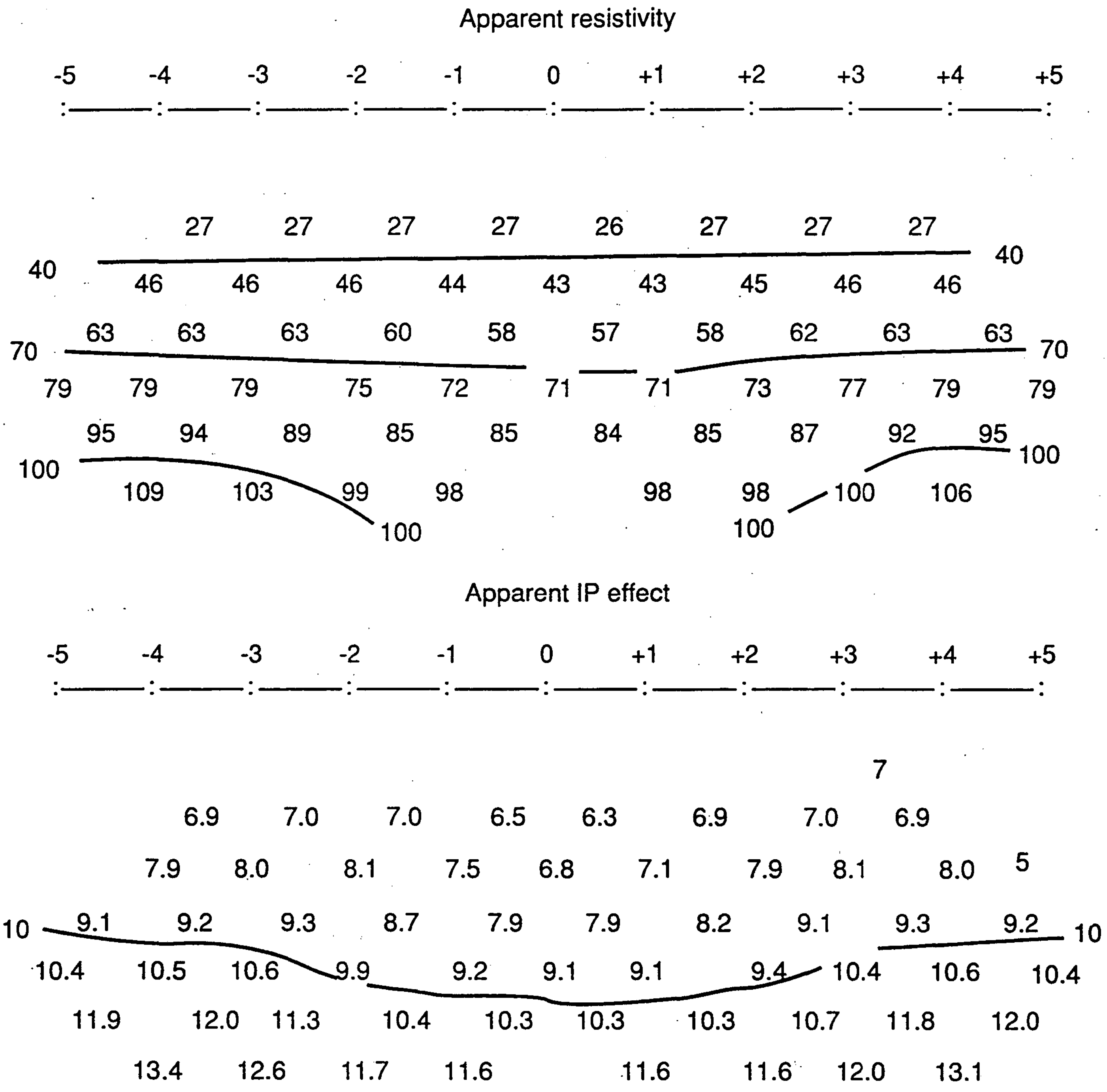

Fig. 11: Numerical model results for Ash-over bedrock with shear zone in bedrock

LAWRENCE BERKELEY NATIONAL LABORATORY
UNIVERSITY OF CALIFORNIA
TECHNICAL & ELECTRONIC INFORMATION DEPARTMENT
BERKELEY, CALIFORNIA 94720